Effects of Temperature on Membrane Electrodiffusion

Oscar Patterson[1], **Ilyssa Summer**[2], **Ramón Martínez**[3]. **Jose Barrios** [1]

[1] Montclair State University, NJ, USA, [2] Arizona State University, AZ, USA, [3] Universidad de Sonora, Hermosillo, México.

Abstract

From a theoretical point of view many cell functions such as regulation of transmembrane concentrations, action potential generation and signaling in general depend on molecular transport across their membrane. In this work we aim to increase our understanding of how the properties of membrane transport depend on temperature. To address this problem, we take a biophysical approach to model molecular flow across the membrane. We model two processes of high relevance: cellular excitability and regulation of extracellular pH. We specifically address the following questions: does temperature affect the dynamics of action potential generation? What is the dependence of the transmembrane acidity levels on body temperature? One potentially interesting aspect of our findings in regard to pH regulation is to unravel mechanisms explaining why temperature-based therapies work for the treatment of some cancers.

1. Flux due to Diffusion and Electric Force

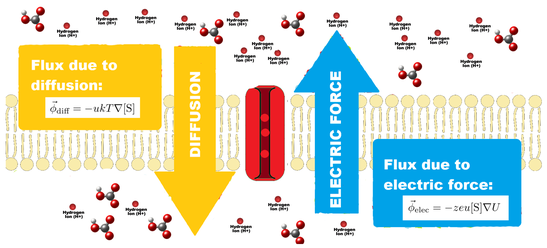

Figure 1: *Transmembrane ionic flux through a channel is determined by diffusion from higher to lower concentrations and by drift in an electric field.*

- **Nernst-Planck Equation:** For an ion species S with concentration [S], the flux through an S-specific channel is

$$\phi_x = -ukT\exp\left(-\frac{zeU}{kT}\right)\frac{d}{dx}\left[[\text{S}]\exp\left(\frac{zeU}{kT}\right)\right]. \tag{1}$$

- **Nernst Potential:** The transmembrane potential difference at which net flux is zero, given by

$$v_{\text{S}} = U_{in} - U_{out} = \frac{kT}{zq}\ln\frac{[\text{S}]_{out}}{[\text{S}]_{in}}. \tag{2}$$

1.1 General expression for flux across the membrane

$$I_x = A_x\sinh\left[\frac{q}{2kT}f(v, z_x, v_x)\right], \tag{3}$$

1.2 Ion channel current

For an S-specific channel of length d and cross-sectional area $A = A(x)$, where x is axial distance, the current I is x-independent and related to ϕ_x by $I = ze\phi_x A(x)$. It follows by (1) that

$$I = \frac{2zeukT}{Q}\sqrt{[\text{S}]_{\text{out}}[\text{S}]_{\text{in}}}\sinh\left(\frac{ze(U_{\text{in}} - U_{\text{out}} - v_{\text{S}})}{2kT}\right), \tag{4}$$

$$\text{where } Q = \int_{\text{in}}^{\text{out}}\frac{1}{A(x)}\exp\left(\frac{ze(U - U_{\text{avg}})}{kT}\right)dx. \tag{5}$$

Assuming $U = U(x)$ is linear, and that $A(x)$ equals the constant A_0 except for a sufficiently small, narrow pore at the channel center of area $A_p << A_0$ and length ϵd, we may approximate Q by $\epsilon d/A_p$, to obtain

$$I = k_{\text{S}}\sinh\left(\frac{ze(v - v_{\text{S}})}{2kT}\right), \quad \text{where } k_{\text{S}} = 2zeukT\sqrt{[\text{S}]_{\text{out}}[\text{S}]_{\text{in}}}\frac{A_p}{\epsilon d}. \tag{6}$$

Here, k_{S} is independent of the membrane potential v. We use (6) as our model for ion channel currents.

1.3 Flux mediated by transporter proteins

Flux through an exchanger $mX_o + nY_i \rightleftharpoons mX_i + nY_o$

$$F = N\lambda(T)\sqrt{[X]_o^m[X]_i^m[Y]_o^n[Y]_i^n}\sinh\left(\frac{q}{2kT}(mz_x(v - v_x) + nz_y(v - v_y))\right), \tag{7}$$

2. Application I: Membrane potential

We consider only the ion channel transport of Na^+ and K^+ ions, using current terms of the form (4).

$$C_m\frac{dv}{dt} = I - A_{\text{Na}}(T)m_\infty(v)^3\sinh\left(\frac{e}{2kT}(v - v_{\text{Na}})\right) - A_{\text{K}}(T)w^4\sinh\left(\frac{e}{2kT}(v - v_{\text{K}})\right) \tag{8}$$

$$\frac{dw}{dt} = \frac{w_\infty(v) - w}{\tau_w(v)}, \tag{9}$$

where

$$\tau_w(v) = \left[2r_w\cosh\left(\frac{z_w e}{2kT}(v_{\text{w}} - v)\right)\right]^{-1}, \qquad w_\infty(v) = \left[1 + \exp\left(\frac{z_w e}{kT}(v_{\text{w}} - v)\right)\right]^{-1},$$

where w is a gating variable representing the proportion of open K^+ channels with time constant $\tau_w(v)$ and steady state $w_\infty(v)$. The Na^+ gating kinetics are assumed to be at quasi-steady state with $m_\infty(v)$ having the same functional form as w_∞.

2.1 Membrane currents

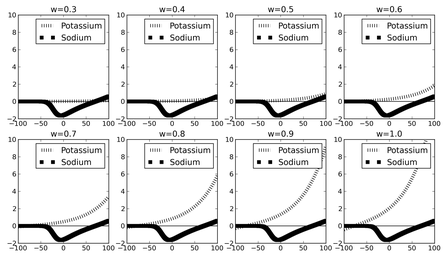

Figure 2: *Potassium (dashes) and sodium current (thick black) amplitudes for different values of the gating variable w. We see that the potassium current is always positive for potential values greater than $v_K \approx -80$ and that as w increases (the proportion of open channels increases) the maximum amplitude of the current increases.*

2.2 Dependence on the rate of opening of potassium channels r

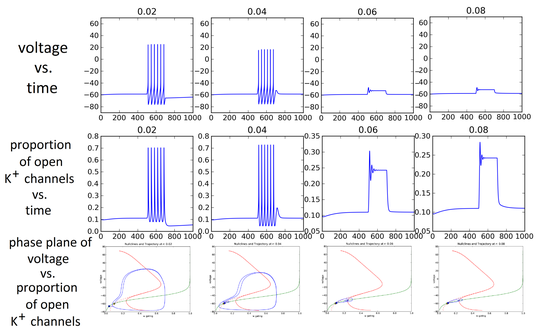

Figure 3: ***Plots of voltage vs. time for different values of*** r. *Each column shows simulations for one value of r. The first two rows show the time-dependent behavior of v and w, respectively. The last row shows the dynamics of the system in phase space.*

2.3 Bifurcation analysis with respect to T

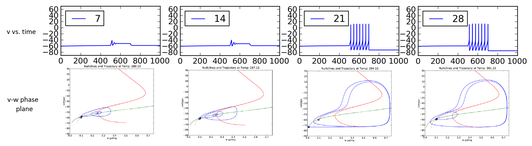

Figure 4: *Simulations for a fixed value of r near it's bifurcation value, for various temperatures. Changes in temperature alone are enough to produce oscillations.*

3. Application II: Transmembrane regulation of pH

3.1 Microenvironment acidity

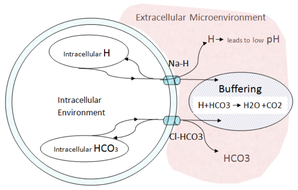

Figure 5: *The buffering of extracellular pH levels through the H^+/HCO_3^- reaction.*

3.2 pH changes as a function of temperature

The system variables are extracellular hydrogen, $[H^+]_o$, and extracellular bicarbonate $[HCO_3^-]_o$ concentrations in the extracellular environment, which will be written for simplification as x and y respectively. The dynamics of the system take the form:

$$\frac{dx}{dt} = N_{Na,H}\lambda_1(T)\,\Psi_x\sinh\left[\frac{q}{2kT}(-v_H + v_{Na})\right] - P(T)x\,y \tag{10}$$

$$\frac{dy}{dt} = N_{Cl,HCO_3}\lambda_2(T)\Psi_y\sinh\left[\frac{q}{2kT}(-v_{HCO_3} + v_{Cl})\right] - P(T)x\,y \tag{11}$$

where

$$\Psi_x = \sqrt{x[Na^+]_0\,[H^+]_i\,[Na^+]_i}, \quad \Psi_y = \sqrt{y[Cl_0^-][HCO_3^-]_i[Cl^-]_i}, \quad \lambda_j(T) = \frac{B_j}{1 + e^{\theta_j(-T + T_{hj})}}$$

The parameters $N_{Na,H}$, N_{Cl,HCO_3} denote, respectively, the number of Na^+/H^+ and Cl^-/HCO_3^- transporters. The factors $\lambda_j(T)$ are the baselines of the transportation rate in terms of empirically determined constants B_j, θ_j and T_{hj} of the transporter protein, while $P(T) = A\exp(-E_a/RT)$ is the Arrhenius rate of the H^+/HCO_3^- reaction.

The system has only one equilibrium point (x^*, y^*) with $x > 0, y > 0$. Throughout the first quadrant, the determinant of the Jacobian matrix is positive, and the trace is negative. The equilibrium point is a stable. T_h, θ_1, $r = N1/N2$ and E_a parameters.

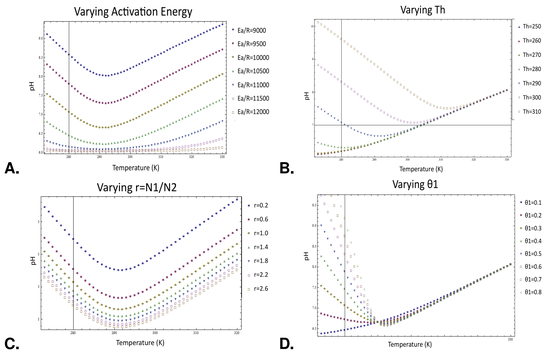

Figure 6: ***pH varies with Temperature.*** ***A.*** *pH-T curves for various E_a.* ***B.*** *pH-T curves for various T_h.* ***C.*** *pH-T curves as a function of r.* ***D.*** *pH-T curves for various θ_1.*

Observations

- Increasing activation energy lowers the extracellular pH values (Fig. 6**A**
- For $T = T_h$ we have maximum acidity in the system. The greater T_h the more acidic the extracellular environment becomes (Fig. 6**B**.
- Increasing the number of Na^+H^+ exchangers lowers the extracellular pH (Fig. 6**C**.
- Increasing θ_1 makes the slope of $pH(T < T_h)$ steeper. For large θ_1, an small decrease in T greatly increases pH (Fig. 6**D**.

3.3 Sensitivity analysis

Sensitivity analysis for the parameters T, $T_h, \theta_1, N1$ and E_a.

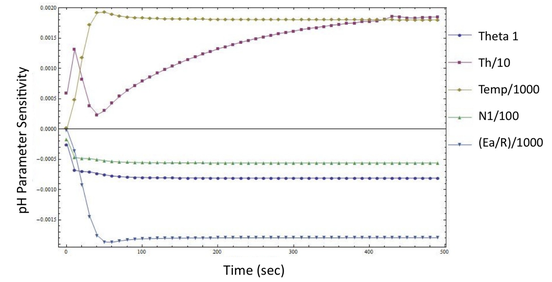

Figure 7: ***pH sensitivity curves***

- It is assumed that in standard conditions, the extracellular environment would be described by a point in parameter space $P_o = (T, T_h, \theta_1, N1, \frac{E_a}{R}) = (310K, 290K, 0.3, 500, 10^4K)$. At this point the the pH regulation system is more sensitive to changes in T and E_a.

4. Conclusions

- **Application 1:** Temperature is typically assumed constant in excitable cell studies. Our primary purpose was to see how temperature, T, affects membrane potential. We studied variations of the system with respect to the basal rate of opening in potassium channels, r. Temperature can trigger sustained oscillations depending on the value of r. If r is sufficiently small ($r < 0.045$ in this example), there can be oscillations, whereas if r is large enough ($r > 0.045$), T fails to produce sustained spiking. We also studied the behavior of the system as T increases while keeping r constant. Our simulations show that transitions between oscillatory non-oscillatory behavior depend can be triggered by changing T.
- **Application 2:** Temperature was found to be fundamental in pH regulation. However, depending on the values of the other parameters, the change in temperature has different impacts on acidity levels. pH increases as the ratio of transporters, $N1/N2$, decreases. This result generates experimentally testable hypotheses as $N1$ can be altered pharmacologically by transport inhibitors. We also found that decreasing activation energy, E_a, increases pH. This can happen, for instance, if the extracellular buffering capacity is pharmacologically increased.

5. Acknowledgments

Financial support: National Science Foundation (NSF - Grant DMPS-0838705); National Security Agency (NSA - Grant H98230-09-1-0104); Alfred P. Sloan Foundation; and the President and Provost Offices at Arizona State University. The Mathematical and Theoretical Biology Institute is now hosted at the Mathematical, Computational and Modeling Science Center at ASU.

We would like to thank Marco Herrera-Valdez (SOLS-MCMSC, ASU) and Mayteé Cruz-Aponte (MCMSC, ASU) for mentoring this work and our MTBI executive director Carlos Castillo-Chavez (MCMSC, ASU).